Received: 2 November 2024 | Revised: 25 January 2025 | Accepted: 9 February 2025

DOI: 10.1002/pc.29706

RESEARCH ARTICLE

spe INSPIRING PLASTICS PROFESSIONALS Polymer COMPOSITES WILEY

Impact of basalt powder on the rheological, thermal, mechanical, and tribological properties of natural and polychloroprene rubber composites: A study on aging and filler interaction

Enes Yildiz[1] | **Talha Degirmenci**[1] | **Melih Esen**[1] | **Mert Goksuzoglu**[2] | **Gozde Kuru**[2] | **Volkan Eskizeybek**[3] | **Emine Feyza Sukur**[1]

[1]Department of Mechanical Engineering, Faculty of Engineering and Natural Sciences, Samsun University, Ondokuzmayıs, Turkey

[2]SAMPA Automotive R&D Center, Samsun, Turkey

[3]Department of Materials Science and Engineering, Faculty of Engineering, Canakkale Onsekiz Mart University, Canakkale, Turkey

Correspondence
Emine Feyza Sukur, Department of Mechanical Engineering, Faculty of Engineering and Natural Sciences, Samsun University, Ondokuzmayıs, Samsun 55420, Turkey.
Email: efeyza.sukur@samsun.edu.tr

Funding information
Scientific and Technological Research Council of Turkey, Grant/Award Number: Project Ref. No: 1139B412301068

Abstract

This study investigates the effects of basalt powder (BP) as a filler in natural rubber (NR) and synthetic polychloroprene rubber (CR) composites, focusing on their structural, mechanical, and thermal properties before and after aging. The NR/BP and CR/BP composites were prepared with varying basalt content levels of 0, 5, 10, 15, 50, and 100 parts per hundred rubber (phr) and characterized accordingly. Mechanical properties such as tensile strength, Young's modulus, and abrasion resistance were evaluated, alongside thermal properties, using thermogravimetric analysis. The results showed that increasing the basalt content reduced dispersion quality and weakened the filler and matrix interaction, decreasing tensile strength and Young's modulus. The reduction in tensile strength is substantial, with a decrease of 71.7% in NR/BP composites and 64.1% in CR/BP composites at maximum additive ratios. Aging significantly improved the tensile strength and modulus of the materials, which are attributed to an increased crosslink density and the transformation of polysulfide bonds into disulfide bonds. Shore A hardness increased with basalt content, reaching 60.3 for NR/BP and 74.1 for CR/BP at 100 phr, while abrasion resistance decreased, with abrasion loss rising by 130% and 88% for NR/BP and CR/BP composites, respectively. Scanning electron microscopy (SEM) analysis revealed increased surface roughness and filler aggregation at higher basalt contents, contributing to reduced mechanical performance. Fourier-transform infrared spectroscopy (FTIR) and energy-dispersive X-ray spectroscopy (EDX) analyses confirmed the presence and dispersion of basalt powder within the composites.

Highlights

- Basalt powder was evaluated as a filler in natural and synthetic rubber composites.

- Increasing basalt content reduced mechanical performance due to filler aggregation.
- Aging enhances tensile strength and modulus, possibly due to increased crosslink density.
- Abrasion resistance significantly worsened with increased basalt loading.
- Basalt powder serves the function of a filler rather than that of reinforcement in rubber.

KEYWORDS

aging, basalt powder, filler interaction, natural rubber, polychloroprene rubber

1 | INTRODUCTION

Eliminating the environmental impact while maintaining high performance is essential for the automotive industry to meet its carbon footprint reduction targets. Achieving these goals depends on adopting sustainable and eco-friendly material solutions. Various parts' diverse performance requirements and loading conditions necessitate the use of specialized materials within the automotive sector. For example, elastomers are among the most cost-efficient materials for addressing noise, vibration, and harshness challenges.[1] Among elastomers, natural rubber (NR) is widely utilized in automotive applications due to its exceptional durability and low compressibility. An additional advantage of NR is its ability to undergo low-temperature processing while offering tunable mechanical properties through strain-induced crystallization.[2] Natural rubber presents several limitations despite these benefits, such as inadequate wear resistance, subpar fatigue performance, and a low modulus. Furthermore, it's thermal, mechanical, tribological, and viscoelastic characteristics require improvement to meet the demands of various components.[3]

Rubber composites enhanced with various fillers can address many of the previously mentioned drawbacks. Creating reactive functional groups through suitable chemical modifications of the rubber can significantly improve its resistance to flames, oils, and solvents.[4] These functional groups also enhance compatibility with the fillers, resulting in better performance of the rubber composites. Fillers play a crucial role in improving rubber's damping properties (hysteresis) and enhancing its rheological, thermal, mechanical, and tribological characteristics by modifying the linear viscoelastic range of the composites.[5,6] While a wide range of organic and inorganic fillers has been explored in research and commercial applications,[7–9] carbon black (CB) remains the most widely used filler in rubber formulations.[10] However, CB production, which relies on petroleum derivatives and involves burning fossil fuels, raises significant environmental concerns. Additionally, the high cost of CB and the limited production capacity in supplier countries could lead to supply chain risks in the future.[3] Recently, several mineral-based agro-industrial residues have emerged as potential eco-friendly alternatives to CB for reinforcing rubber. These include materials such as eggshells (eggshell powder and mica), inorganic powders (e.g., silica, nanoclay), and chopped natural fibers (e.g., hemp, flax).[11,12] Incorporating recyclable and environmentally friendly natural fibers, like hemp fibers, into polymers offers reduced weight, improved high-temperature resistance, and enhanced mechanical properties.[13] However, despite their lightweight nature, hemp reinforcements in rubber are limited due to challenges in achieving sufficient compatibility and adhesion with the rubber matrix. Furthermore, optimizing the properties of hemp fibers often requires additional chemical or physical treatments, which can constrain their application as a reinforcement material in rubber.[14]

Basalt reinforcements, derived from melting natural basalt stones, have become increasingly popular due to their environmentally friendly nature and outstanding properties. These include high strength, excellent electrical, thermal, and sound insulation, and resistance to heat, wear, and corrosion—all achieved relatively cheaply.[15–18] Research has highlighted the significant influence of basalt fiber (BF) reinforcements on rubber's vulcanization and dynamic mechanical properties. For example, integrating BF into natural and styrene-butadiene rubber (SBR) composites can considerably reduce scorch and vulcanization times.[19,20] Additionally, basalt fillers with flake and fiber morphologies have been shown to enhance thermal stability and decrease the flammability of silicone rubber (SR) composites.[21] Wu and Feng demonstrated that the mechanical properties of fluoro rubber are optimized by reinforcing it with short basalt fibers, specifically with a composition of 100 phr fluoro rubber, 10 phr short basalt fiber, and 2.5 phr KH-550 coupling agent.[22] Furthermore, Li et al. explored

the effect of coupling agents on the adhesion between basalt fibers and NR/SBR matrices. Their findings revealed that (3-aminopropyl) triethoxysilane was the most effective in improving interfacial fatigue performance by enhancing the matrix's initial adhesion, stress distribution, and fatigue properties.[23] Rybiński et al. reported that basalt fillers, whether in flake or fiber form, significantly enhance the thermal properties and reduce the flammability of silicone rubber composites.[24] Their subsequent study evaluated the impact of basalt and carbon fillers on ethylene-propylene-diene (EPDM) composites. Although basalt fillers effectively reduced the thermal decomposition rate, they did not significantly improve the tensile strength of EPDM. This limitation was attributed to the agglomeration and misalignment of basalt fibers within the rubber matrix, adversely affecting mechanical properties.[25]

Existing literature reveals a limited focus on integrating basalt into rubber materials, with most studies concentrating on basalt in its fiber form. This study addresses this gap by developing cost-effective and sustainable composite materials reinforced with basalt powder in natural and synthetic chloroprene rubber. Various basalt powder ratios were utilized to investigate their effects on the properties of NR and CR composites, alongside a detailed examination of their behavior under aging conditions. The findings provide valuable insights into the combined impact of basalt reinforcement, filler content, and aging on rubber composites' rheological, thermal, mechanical, and tribological characteristics.

2 | EXPERIMENTAL PROCEDURE

2.1 | Materials

In this study, two different types of rubber were utilized. Vietnamese Natural Rubber SVR CV 60 (Mooney viscosity ML 1 + 4 (100°C) 60) was obtained from Dakruco, and a general-purpose mercaptan-modified polychloroprene rubber (SN-232 from Wealth Ocean) with a medium crystallization rate was used as the synthetic rubber. N550 (OMSK Carbon Group) was used as a filler, a commonly used carbon black grade in the rubber industry. The study also used basalt powder as a filler obtained from Aydınlar Madencilik. Treated distillate aromatic extracts (TDAE from Petrofer) were used as a rubber processing oil with high aromatic content. It served as a rubber-softening additive in the formulations. Dioctyl phthalate (DOP) was obtained from the Plastifay Chemical Industry and used as a softening agent to increase the processibility of synthetic rubber compounds. Stearic acid, zinc oxide, and magnesium oxide were activated in rubber formulations. The melting point of stearic acid is 67–69°C, and the specific gravity is 0.838 g. cm^{-3}. The purity of ZnO fine powder was 99%, and the specific gravity was 5.6 g/cm^{-3}. Antilux 111, 4010, and TMQ were used as anti-aging additives. S 80 and sulfur were used as vulcanization agents. TBBS 75 and ETU 80 were used as accelerators.

Six compounds were prepared for each rubber type to investigate the impact of basalt powder on rheological, mechanical, thermal, and tribological properties. NR-based and CR-based formulations containing 5–100 phr basalt powder have been prepared and are represented in Tables 1 and 2, respectively. The N550 concentration was fixed at 50 phr for all formulations, and only the basalt powder concentration was altered.

2.2 | Preparation of the compounds

Rubber composites were prepared using a 1.5-L intermeshing laboratory mixer from Harburg Freudenberger Mixing Group (HF MG brand, Germany). For the natural rubber composite masterbatches, SVR CV 60, N550, basalt powder, TDAE, and other specified ingredients in the developed formulations were mixed at an initial temperature of 70°C for approximately 8 min. Subsequently, S80 and TBBS 75 were incorporated into the masterbatch. The rotor and chamber temperatures were regulated during mixing using a Temperature Control Unit (TCU). SN232, N550, basalt powder, DOP, MgO, and stearic acid were combined to produce chloroprene-based composite masterbatches. After 24 hours, active zinc oxide, sulfur, and ETU were added to the masterbatch.

2.3 | Dynamic viscosity analysis

The dynamic shear viscosity of each formulation was measured to assess its processability, consistency, curing efficiency, performance prediction, and optimization of the rubber compounds. Approximately 5 g samples were obtained from each formulation using a volume cutter, and the viscosity was analyzed with an RPA2000 Rubber Process Analyzer from Alpha Technologies. The tests were conducted at 100°C, with a strain angle of 1% and a frequency of 33 Hz.[26]

2.4 | Cure characteristics

The rubber process analyzer (*RPA*) assesses the viscoelastic properties of elastomers, providing critical data on their

TABLE 1 Filled natural rubber compound formulations in phr.[a]

Materials (phr)	Formulations					
	NR/BP 0 phr	NR/BP 5 phr	NR/BP 10 phr	NR/BP 15 phr	NR/BP 50 phr	NR/BP 100 phr
SVR CV 60	100	100	100	100	100	100
N 550	50	50	50	50	50	50
Basalt powder	-	5	10	15	50	100
TDAE	5	5	5	5	5	5
Zinc oxide	5	5	5	5	5	5
Steraic acid	1.5	1.5	1.5	1.5	1.5	1.5
Antilux 111	2	2	2	2	2	2
4010	2	2	2	2	2	2
2,2,4-Trimethyl-1,2-Dihydroquinoline (TMQ)	1	1	1	1	1	1
TOTAL phr	166.5	171.5	176.5	181.5	216.5	266.5
S 80	2	2	2	2	2	2
TBBS 75	2	2	2	2	2	2

[a]phr, parts per hundred rubber.

TABLE 2 Filled chloroprene rubber compound formulations in phr.[a]

Materials (phr)	Formulations					
	CR/BP 0 phr	CR/BP 5 phr	CR/BP 10 phr	CR/BP 15 phr	CR/BP 50 phr	CR/BP 100 phr
SN 232	100	100	100	100	100	100
N 550	50	50	50	50	50	50
Basalt powder	-	5	10	15	50	100
DOP	5	5	5	5	5	5
MgO	5	5	5	5	5	5
Steraic acid	1	1	1	1	1	1
TOTAL phr	161	166	171	176	211	261
Active ZnO	4.5	4.5	4.5	4.5	4.5	4.5
Sulfur	1	1	1	1	1	1
ETU 80	0.4	0.4	0.4	0.4	0.4	0.4

[a]phr, parts per hundred rubber.

processability and curing characteristics.[27] Parameters such as maximum torque (M_H), minimum torque (M_L), scorch time (t_{S2}), and optimum cure time (T_{s90}, the time required for the torque to reach 90% of its maximum value) were determined using cure curves obtained from a moving die rheometer (Alpha Technologies RPA2000 Rubber Process Analyzer) at 180°C, as specified by ASTM D 5289. Additionally, the cure rate index (*CRI*), which reflects the curing rate, was calculated based on Equation (1).[28]

$$\mathrm{CRI} = 100/(\mathrm{T_{s90}} - \mathrm{t_{S2}}) \quad (1)$$

2.5 | Characterizations

The tensile test was conducted according to ASTM D412-16 using a Zwick Roell Z010 testing instrument. The cross-head speed was set to 200 mm/min, and all tests were performed at room temperature. Five specimens, each with a thickness of 2 mm, were prepared and tested for each compound formulation. Hardness measurements were carried out by ASTM D1415, with three measurements taken for each compound. The average of these values was reported as the hardness.

To assess the aging performance of each compound, the test samples underwent accelerated aging at 70°C for 72 h in an Elastocon Cell Aging Oven, which contains six cells.

Infrared spectra were collected to analyze the impact of basalt powder content on the compounds. Spectra for the twelve prepared compounds were obtained at 25°C with a resolution of 4 cm^{-1} in the wavelength range of 600–4000 cm^{-1}, using a Perkin Elmer Fourier Transform Infrared Spectrometer Spectrum II. Specimens, each at least 2 mm thick, were placed in the spectrometer's test compartment for analysis.

Thermogravimetric analysis (TGA) was carried out using a Perkin Elmer Pyris 1 Thermogravimetric Analyzer. Approximately 5–15 mg of each of the twelve compounds was analyzed by heating the samples at a constant rate. The samples were heated from 0 to 600°C in a nitrogen atmosphere and from 600 to 900°C in an oxygen atmosphere. The mass loss was recorded as a function of temperature, and the impact of basalt powder content on the thermal decomposition temperature of the compounds was assessed based on the results.

Abrasion tests were performed according to ASTM D5963, which outlines the methodology for determining the abrasion resistance of rubber materials. Abrasion resistance was measured by moving a sample across an abrasive surface mounted on a rotating drum and expressed as volume loss in mm^3 or as an abrasion resistance index (%). Lower volume loss values indicate better abrasion resistance. Each sample was weighed before and after the test, and the volume loss in mm^3 was calculated using the formula provided in the standard. Three samples were tested for each compound, and the average values were reported.

3 | RESULTS AND DISCUSSION

3.1 | Rheological properties of NR/BP and CR/BP composites

Table 3 illustrates the effect of basalt concentration on the rheological properties of NR/BP and CR/BP composites. In NR/BP composites, increasing basalt concentration from 0 to 5 phr results in a 9.94% increase in viscosity. This rise can be attributed to the basalt powders restricting the movement of the rubber matrix. When the concentration is further increased from 5 to 10 phr, there is a more substantial increase of 15.4%, indicating that the interactions between the powders are intensifying, which leads to a further enhancement of viscosity. However, when the concentration is raised from 10 to 15 phr, a slight decrease of 1.2% occurs, suggesting that the basalt powders may start to agglomerate at this stage. From 15 to 50 phr, we observe a significant reduction of 14.2%, implying that the basalt powders may hinder interactions between the rubber chains at higher concentrations, resulting in increased fluidity. Finally, when the concentration rises from 50 to 100 phr, there is a 5.4% increase in viscosity, indicating that at very high concentrations, the basalt powders can once again restrict the movement of the rubber matrix.

In the CR/BP composites, the viscosity increases slightly by 0.92% as the concentration of basalt powders rises from 0 to 5 phr. This suggests that the basalt powders begin to interact with the CR matrix. When the concentration is increased from 5 to 10 phr, a more noticeable rise of 3.33% indicates that the powders are becoming more widely dispersed within the CR matrix, which further increases viscosity. As the concentration increases from 10 to 15 phr, the viscosity rises by 4.91%, suggesting that the basalt powders strongly interact with the CR matrix, which enhances viscosity even more. When the concentration increases from 15 to 50 phr, a significant increase of 18.03% is observed, implying that the basalt powders impede movement within the CR matrix even further at higher concentrations. Finally, when the concentration rises from 50 to 100 phr, the viscosity jumps by 50.1%, indicating that the basalt powders become densely packed within the CR matrix, severely restricting fluidity.

The viscosity values measured for the prepared compounds are presented in Table 3. For the NR/BP compounds, the viscosity initially increases as the BP content rises to 10 phr but then decreases at 15 phr and continues to decline at higher BP contents (50 and 100 phr). In contrast, the viscosity of CR/BP composites consistently increases with higher BP content, suggesting a different interaction between CR and BP compared to NR. Generally, an increase in filler loading is expected to result in higher viscosity. When examining the viscosity results, it can be concluded that filler-filler interaction

TABLE 3 Viscosity values of NR/BP and CR/BP composites.

	*n**@33 Hz Pa.s					
Samples	**0 phr**	**5 phr**	**10 phr**	**15 phr**	**50 phr**	**100 phr**
NR/BP composites	2083	2290	2404	2058	1787	1970
CR/BP composites	6295	6353	6505	6604	7430	9448

is more pronounced in the CR/BP compounds than in the NR/BP compounds. NR/BP compounds have a more significant interaction between the rubber and the filler, resulting in a higher bound rubber content due to the more effective interaction between basalt powders and natural rubber.

In addition to viscosity, cure properties have also been obtained using RPA, and the results for all compounds are given in Table 4. The scorch time (t_{s2}) and curing time (T_{s90}) refer to the initiation and completion of vulcanization processes, respectively.[29] M_L, a measure of torque reflecting uncured rubber viscosity, offers valuable insights into rubber processing performance through its minimum torque.[29,30] M_H indicates the viscosity level attained when the curing process is finished. Chemical crosslinking serves as the primary defining factor in the vulcanization process. The parameter ΔM, derived from the difference between maximum torque (M_H) and minimum torque (M_L), effectively illustrates the degree of chemical crosslinking.[30–32] The cure rate index (*CRI*) measures the vulcanization rate derived from the differences between cure and scorch times. It is found as 100 divided by the difference between cure and scorch times.[29]

It can be observed from the RPA data that there is no significant change in curing parameters such as t_{s2}, T_{s90}, and M_L as a result of adding basalt powder into natural rubber and chloroprene rubber compounds. It can be extracted from RPA results that there is a critical change in M_H data only in CR compounds. There is a linear increase in M_H values in CR/BP compounds up to 57% between compounds CR/BP 100 phr and CR/CP 0 phr. This increase can be associated with higher filler –filler interaction in CR/BP compounds. Another fact that shows lower filler-to-filler interaction in NR/BP compounds is that there is no such change in M_H values.

Torque versus time graphs plotted with data from the RPA are presented in Figure 1 for all compounds. Rybinski et al. stated that adding basalt filler has practically no influence on the scorch time values of the silicone rubber compounds.[24] Li et al. obtained that adding basalt fillers did not affect the curing rate, but the maximum torque increased with increases in basalt filler amount.[33] Rybinski et al. presented that adding basalt fillers did not significantly alter the cure parameters of EPDM-based compounds relative to the reference sample.[25]

3.2 | Thermal properties of NR/BP and CR/BP composites

Figure 2 displays the TGA thermograms of NR and CR composites with varying basalt powder loadings. In Figure 2A, the thermograms indicate that the thermal degradation of NR/BP composites occurs in two distinct temperature ranges: 300–450°C, corresponding to the breakdown of natural rubber, and 600–700°C, which is related to the degradation of other components within the composite.[34] In the case of CR/BP composites, as shown in Figure 2B, the TGA thermograms reveal three distinct stages of degradation across the temperature range of 100–800°C. The first stage occurs at temperatures above 250°C and is associated with the thermal decomposition of organic impurities. The second stage, which takes place between 400 and 500°C, is linked to the degradation of polymer chains. Finally, the third stage, observed above 650°C, corresponds to the

TABLE 4 Rheometric parameters of NR/BP and CR/BP composites.

Samples	Minimum torque M_L(dNm)	Maximum torque M_H (dNm)	Torque difference $M_H - M_L$	Scorch time t_{s2} (min)	Cure time T_{s90} (min)	Cure rate index (min^{-1})
NR/BP 0 phr	0.69	12.83	12.14	0.80	1.39	169.49
NR/BP 5 phr	0.72	12.69	11.97	0.79	1.42	158.73
NR/BP 10 phr	0.72	13.69	12.97	0.72	1.38	151.52
NR/BP 15 phr	0.47	14.00	13.53	0.73	1.39	151.52
NR/BP 50 phr	0.29	13.67	13.38	0.90	1.50	166.67
NR/BP 100 phr	0.23	14.95	14.72	0.89	1.41	192.30
CR/BP 0 phr	3.67	21.43	17.76	0.42	3.48	32.68
CR/BP 5 phr	3.69	21.98	18.29	0.42	3.57	31.75
CR/BP 10 phr	3.47	23.36	19.89	0.42	3.64	31.06
CR/BP 15 phr	3.64	24.05	20.41	0.42	3.53	32.15
CR/BP 50 phr	3.65	26.39	22.74	0.39	3.60	31.15
CR/BP 100 phr	4.58	33.62	29.04	0.36	3.55	31.35

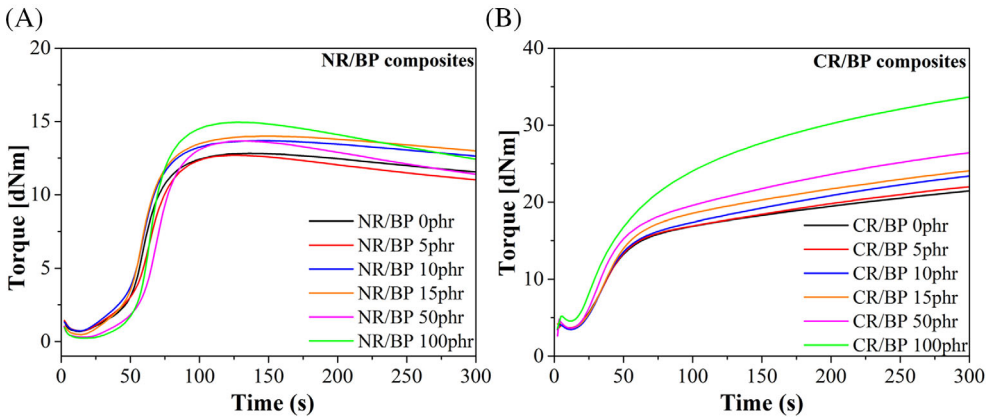

FIGURE 1 Rheometric curves of (A) NR/BP and (B) CR/BP composites.

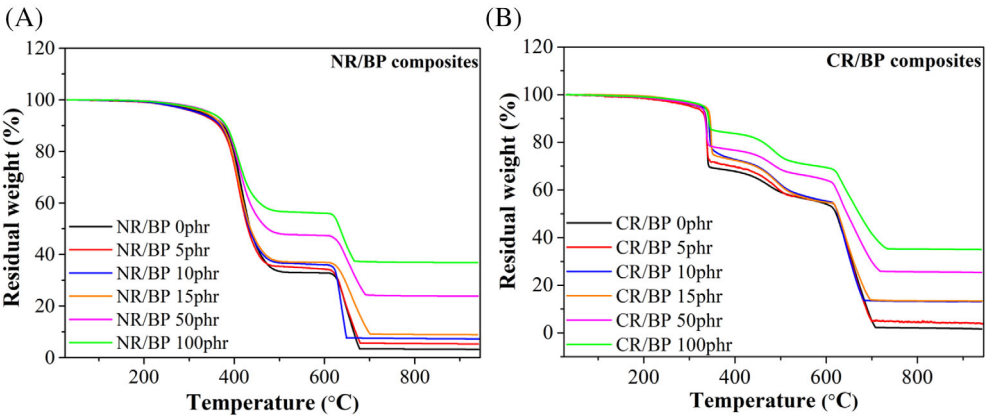

FIGURE 2 TGA thermograms of basalt reinforced composites (A) NR/BP composites and (B) CR/BP composites.

transformation of chars into CO2 as the gas flow transitions from nitrogen to air.[35]

The temperature at which rubber composites lose 50% of their weight (known as T_{50}, in°C) is an essential measure of their thermal stability.[34,36] The results indicate that the T_{50} values of the composites remain relatively unchanged when reinforced with basalt at 5, 10, and 15 phr (Table 5). However, there are noticeable differences in T_{50} values when the basalt reinforcement increases to 50 and 100 phr. For natural rubber and chloroprene rubber composites, thermal stability improves as the basalt content rises, which is evident through higher T_{50} values and more char residue. This effect is particularly pronounced with higher basalt loadings of 50 and 100 phr. For instance, the T50 values for NR and CR composites with 100 phr of basalt powder reach 633.4 and 671.3°C, respectively, marking increases of 45.6% and 7.6% compared to their neat counterparts. Adding basalt powder boosts the thermal degradation resistance of NR composites, showcasing remarkable heat resistance. This enhancement is mainly due to basalt's excellent heat capacity and thermal stability, reaching up to 1200°C.[25] Essentially, basalt acts like a thermal barrier, soaking up the heat and safeguarding the polymer from potential damage and degradation.[24] Moreover, the char residue left behind is another helpful measure for assessing the thermal stability of these composites. The amount of char residue correlates with the temperatures at which weight loss happens, further validating the improved thermal stability as basalt content increases.[37]

3.3 | Fourier transform infrared (FTIR) spectroscopy

FTIR spectra of basalt powder-reinforced NR and CR composites before and after aging are shown in Figures 3 and 4, respectively, and the characteristic bands are given in Table 6. The absorption band in the range of 3400–3700 cm^{-1} correlates to the presence of OH groups of water and mineral acid residues like $[CO_4]^{2-}$, $[SiO_4]^{2-}$ and $[-Al(OH)_4]-$.[38] The peaks detected at 3672 cm^{-1} (Figure 3) and 3678 cm^{-1} (Figure 4) indicate OH groups originating from the basalt content. Additionally, there is an increase in the peaks associated with hydroxyl stress vibrations, which can be attributed to absorbed water.[18] C-H bonds exhibit absorption in the range of 2853–2962 cm^{-1}. The peak observed between 1475 and 1300 cm^{-1} also indicates C-H bending. The peak at 1000–650 cm^{-1} indicates C=C-H bending.[39] The prominent peaks with the most significant

Sample	T_5 (°C)	T_{10} (°C)	T_{50} (°C)	Char residue % (at 800°C)
NR/BP 0 phr	323.3	373.0	435.0	3.4
NR/BP 5 phr	308.2	363.0	429.7	5.5
NR/BP 10 phr	311.1	367.0	432.7	7.5
NR/BP 15 phr	329.2	371.1	435.1	9.0
NR/BP 50 phr	340.8	378.5	471.3	24.0
NR/BP 100 phr	338.9	380.1	633.4	37.0
CR/BP 0 phr	311.5	336.1	623.7	2.1
CR/BP 5 phr	297.0	333.3	625.5	4.5
CR/BP 10 phr	317.9	342.1	624.6	13.3
CR/BP 15 phr	328.2	345.4	626.1	13.5
CR/BP 50 phr	314.3	334.8	644.9	25.7
CR/BP 100 phr	328.5	341.8	671.3	35.2

TABLE 5 Thermal degradation data of NR/BP and CR/BP composites at different weight loss temperatures.

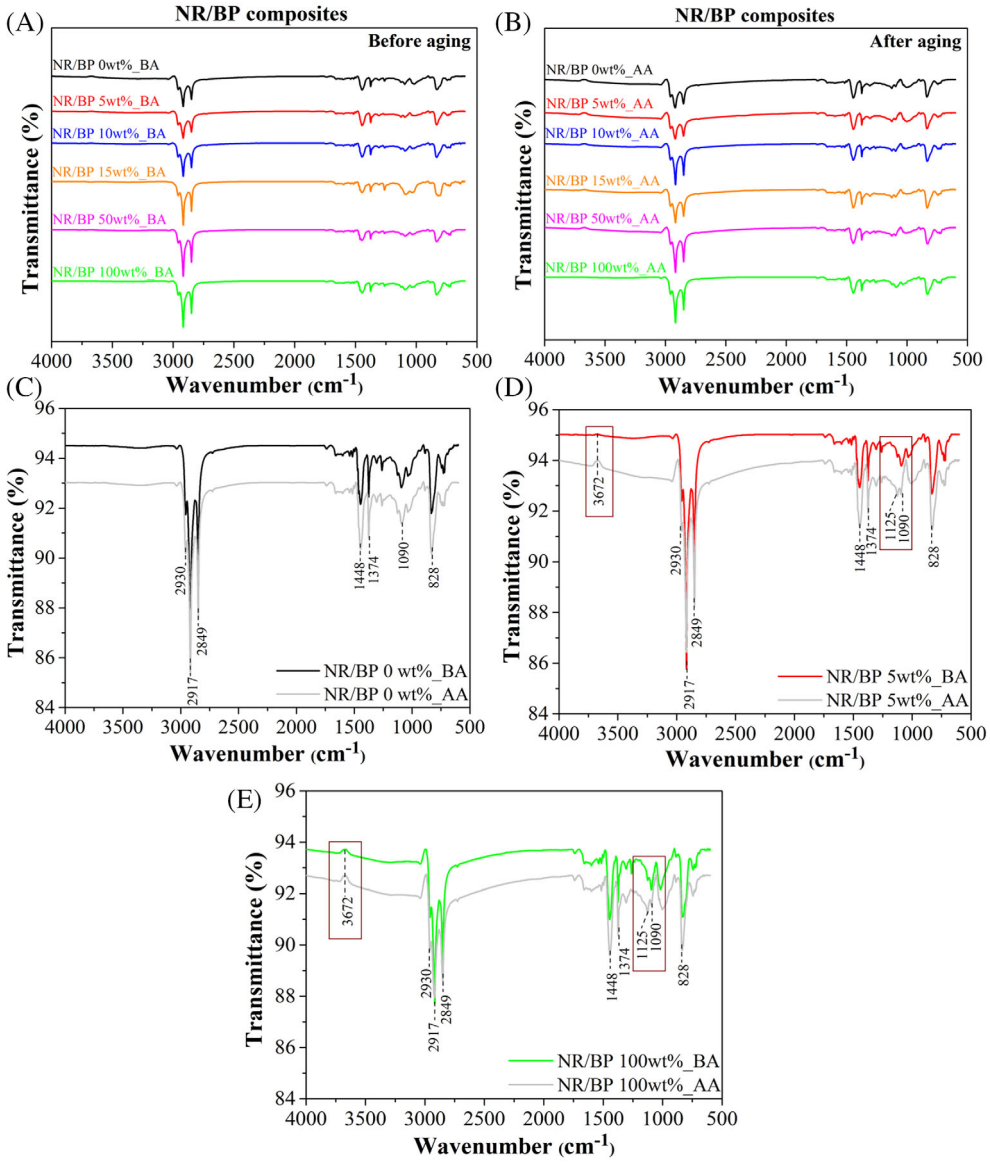

FIGURE 3 FTIR spectra of basalt reinforced NR composites (A) before aging, (B) after aging, (C) NR/BP 0 phr, (D) NR/BP 5 phr, and (E) NR/BP 100 phr.

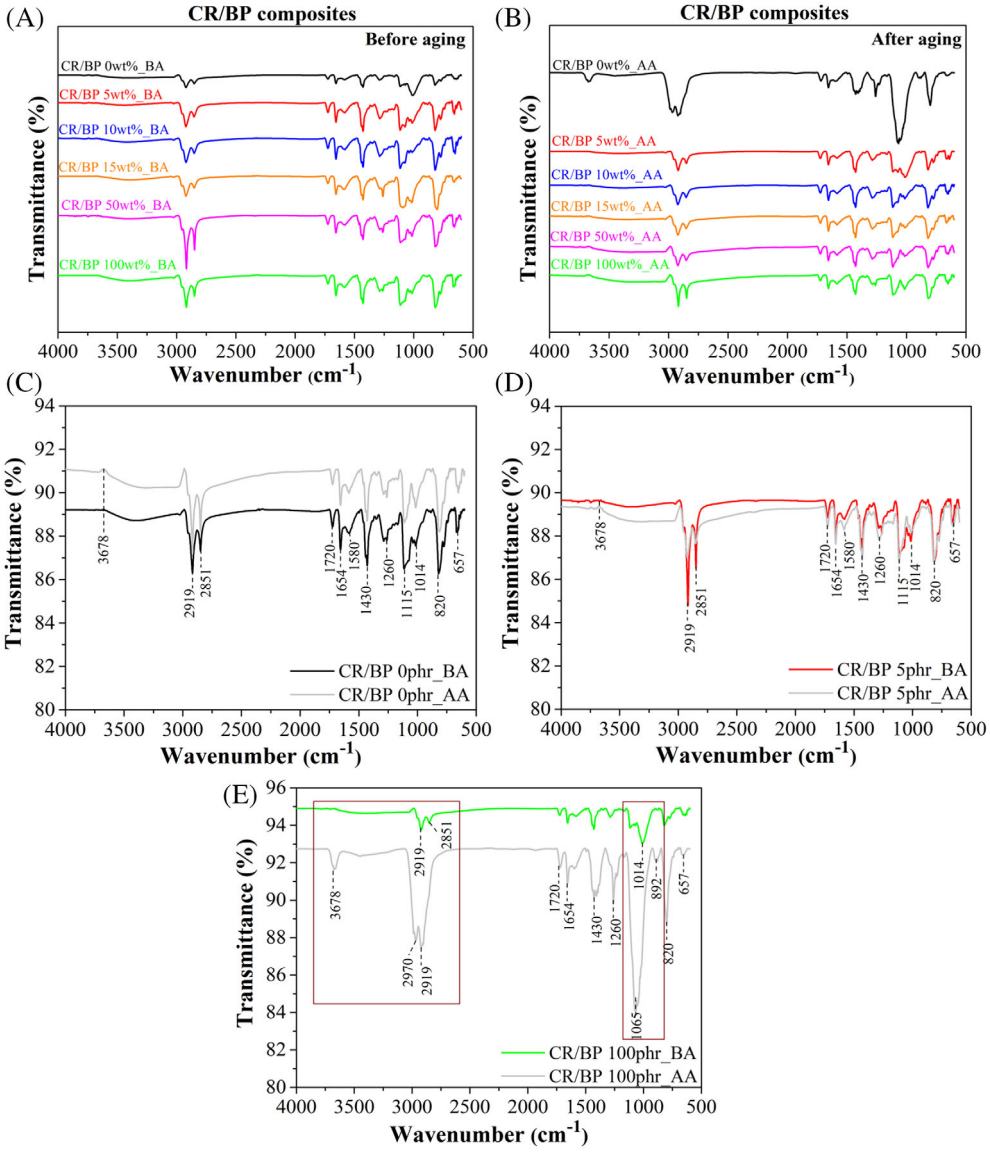

FIGURE 4 FTIR spectra of basalt reinforced CR composites (A) before aging, (B) after aging, (C) CR/BP 0 phr, (D) CR/BP 5 phr, and (E) CR/BP 100 phr.

intensities, observed at 2970, 2930, 2919, 2917, 2851, and 2849 cm^{-1}, are indicative of the stretching vibrations of CH_3, CH_2, and CH groups inside the cis-1,4-polyisoprene macromolecules.[34] Polyisoprene is a polymer composed of isoprene (C5H8) monomers. It is the principal chemical component of both natural and synthetic rubber. The most optimal location for detecting the existence of cis-polyisoprene was the absorption at 2960 cm^{-1} (C-H_3 group) and 1444 cm^{-1} (C-H deformation).[40] The symmetric stretching oscillations, vibrations, and deformations resulting from bending in the 2985–1160 cm^{-1} range are associated with CH_3 and CH_2 groups present in basalt powder.[41] The presence of basalt powder reinforcement is confirmed by detecting a peak at 1125 cm^{-1} in the 5 and 100 phr reinforced NR composites. The accelerated aging process resulted in an augmentation of the OH peak intensity, novel peaks (2970 cm^{-1}) formed, and a slight shift of peaks (1115–1065 cm^{-1}).

3.4 | Mechanical properties of NR/BP and CR/BP composites

The characteristic tensile stress –elongation at break (%) curves of NR and CR composites before and after aging are provided as Data S1. The typical mechanical performance data for NR/BP composites with varying basalt contents is presented in Figure 5. The NR/BP0 composite, which does not contain basalt reinforcement, exhibited the highest tensile strength at 24.8 MPa and an elongation at break of 450%. However, as the basalt content increased from 0 to 100 phr, tensile strength and elongation at break (%) gradually decreased. The lowest tensile strength recorded was 7 MPa for the 100 phr basalt powder content, marking a significant decrease of 71.7% (Figure 5A). The excessive addition of basalt powder beyond 15 phr negatively impacts the tensile load-carrying capacity of the NR matrix, leading to a

TABLE 6 Assignment of the FTIR-obtained bands for NR/BP and CR/BP composites spectra.[42]

Wavenumber (cm^{-1})		
NR/BP composites	**CR/BP composites**	**Assignment of peaks**
3672	3678	OH groups
	2970	Asymmetric $-CH_3$ stretching
2930		Asymmetric $-CH_2-$ stretching
2917	2919	Symmetric $-CH_3$ stretching
2849	2851	Symmetric $-CH_2$, $-CH_3$ stretching
1654	1654	C=C stretching
1448	1430	$-CH_2-$ stretching $-CH_3$ rocking
1374		Asymmetric $-CH_3$ deformation
1125	1115	C–C stretching $-CH_2-$ wagging
1090		$-CH_2-$ twisting
	1014	C–C stretching
825	820	C=C–H out-of-plane bending (cis-1,4 addition)

pronounced decline in both tensile strength and elongation at break. This phenomenon is primarily attributed to the agglomeration of the basalt powder within the NR matrix as the reinforcement content increases.[16,18] Previous studies have indicated an initial rise in mechanical properties, such as tensile strength, at relatively lower basalt contents.[43,44] In contrast, this study found no increase in tensile strength, even at lower contents beginning from 5 phr, suggesting insufficient compatibility due to the lack of modification. The tensile strength of NR/BP15 composites is approximately 17 MPa, making them suitable for various industrial applications. This formulation saves up to 20% by incorporating 15 phr of basalt powder into the rubber compounds.

The aged composites exhibited higher tensile strength and Young's modulus across all cases than the unaged composites, including the NR/BP0 sample. Kong et al. attributes the enhanced mechanical performance after thermal aging to the increase in total crosslink density over time.[45] During the initial aging process of natural rubber, lower bond energy polysulfide bonds transition into higher energy disulfide bonds, significantly improving mechanical performance. The effects of aging showed a slight impact on tensile strength and elongation at break (Figure 5A,B); however, the tensile strength and elongation at break values of all basalt contents after aging were nearly equal to or greater than the corresponding initial values. Conversely, the effects of aging were more pronounced in the Young's modulus. Specifically, Young's modulus increased for all basalt contents following hydrothermal aging at both 50% and 100% strain (Figure 5C). It was also noted that the difference in Young's modulus before and after aging decreased with increasing deformation.

Tensile strength, elongation at break, and Young's modulus data of CR/BP composites with varying basalt contents are given in Figure 6. Pure CR (without any basalt reinforcement) demonstrated the highest tensile strength, measuring approximately 19.5 MPa and an elongation at a break of 225%. As the basalt content increases from 0 to 100 phr, the tensile strength decreases significantly, especially when compared to NR/BP composites (Figure 6A). At the same time, the elongation at break values remains relatively consistent, ranging from 150% to 200% (see Figure 6B). When the basalt content reaches 100 phr, the tensile strength drops to 7 MPa, and the elongation at break decreases to 175%. This rapid decline in mechanical properties, even with low basalt contents, suggests a greater tendency for basalt powder to agglomerate within the CR matrix than the NR matrix. After the aging process, similar behaviors were observed in the CR/BP composites. The aging process had a limited impact on the mechanical performance of these composites. Surprisingly, the aged composites exhibited higher tensile strength and Young's modulus in all cases, including the pure CR sample. This improvement can be attributed to increased total crosslink density over time. As noted by Kong et al., the initial aging process causes the transformation of lower-energy polysulfide bonds into higher-energy disulfide bonds, leading to enhanced mechanical performance.[45]

The tensile strength and elongation at break exhibited slight variations due to aging; however, for all basalt content levels, the tensile strength and elongation at break values after aging are nearly equal to or higher than the corresponding initial values. Specifically, tensile strength decreases with increasing basalt content before aging, dropping from 19.5 MPa (pure CR) to 7 MPa (100 phr basalt). After aging, the tensile strength values slightly increase across all basalt contents. In contrast, the effect of aging is more pronounced in the Young's modulus (Figure 6C). Young's modulus increased after thermal aging for all basalt contents during 50% and 100% strain measurements. Additionally, it was found that the difference in Young's modulus before and after aging diminishes with increasing deformation. This indicates that the composites become stiffer and less ductile after aging, resulting in improved mechanical performance, particularly in Young's modulus.

3.5 | Tribological properties of NR/BP and CR/BP composites

Figure 7A,B present the Shore A hardness measurements for NR/BP and CR/BP composites before and after aging,

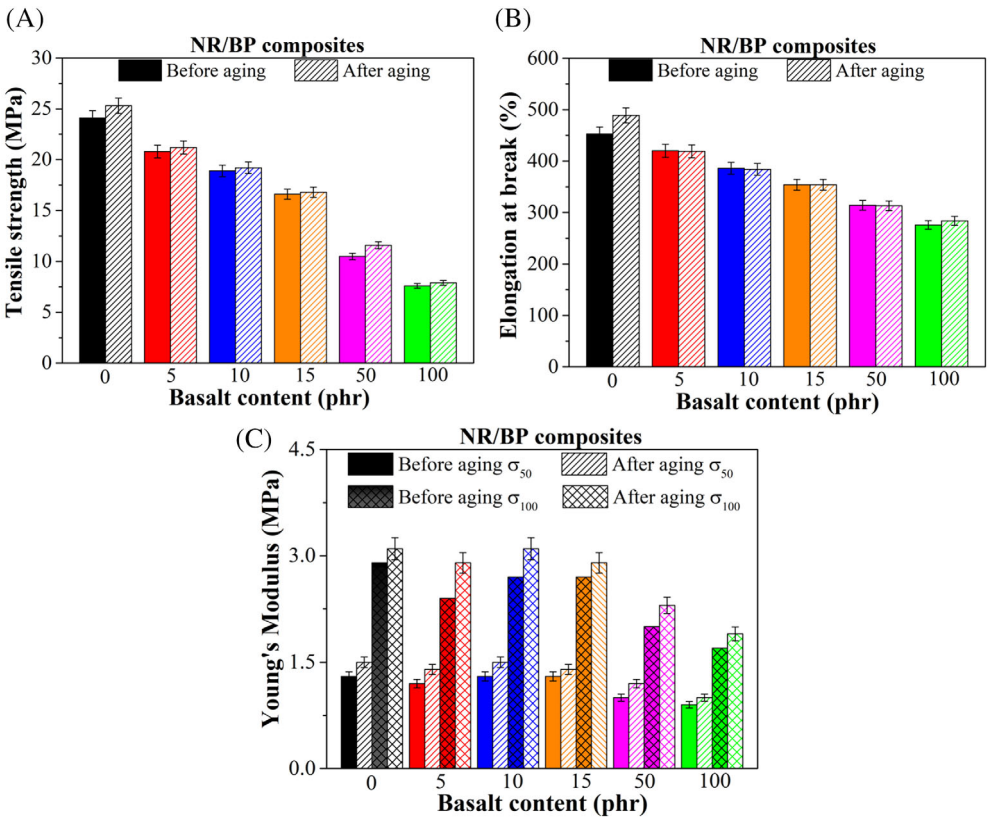

FIGURE 5 Tensile test results of NR/BP composites before and after aging, (A) tensile strength, (B) elongation at break (%), (C) Young's modulus.

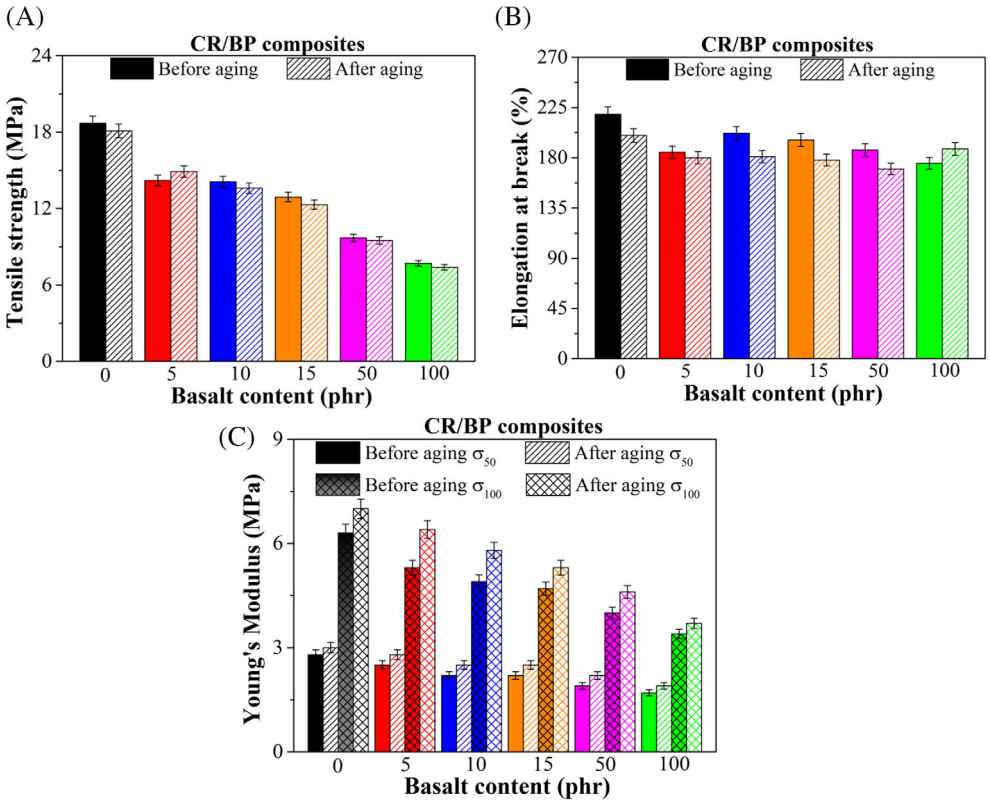

FIGURE 6 Tensile test results of CR/BP composites before and after aging, (A) tensile strength, (B) elongation at break (%), (C) Young's modulus.

respectively. Shore A hardness is a standard method for evaluating the resistance of rubbers and elastomers to indentation; higher values indicate greater hardness, while lower values signify softer materials.[46] For pure natural rubber, the recorded Shore A hardness is 55.4. When natural rubber is combined with basalt powder at

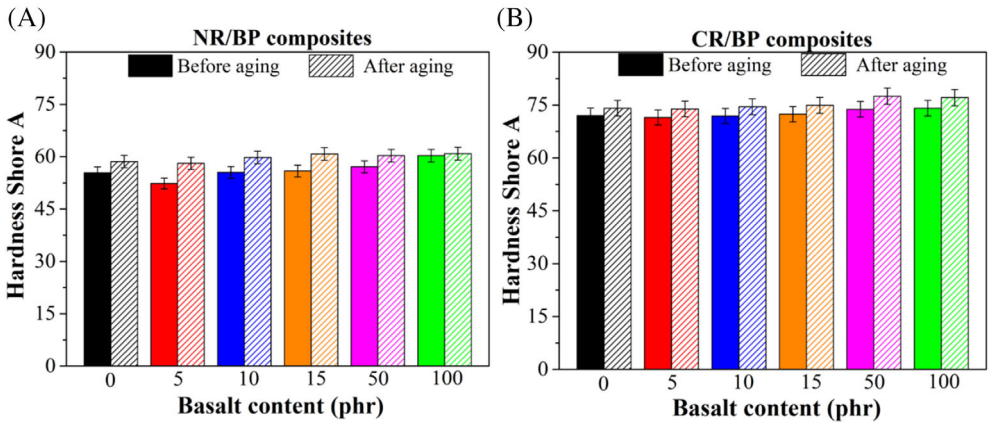

FIGURE 7 Shore A hardness of the (A) NR/BP composites and (B) CR/BP composites at various basalt contents.

Samples	Basalt content					
	0 phr	5 phr	10 phr	15 phr	50 phr	100 phr
NR/BP_Before Aging	55.4	52.3	55.5	55.9	57.1	60.3
NR/BP_After Aging	58.6	58.1	59.8	60.8	60.3	60.9
CR/BP_Before Aging	72	71.5	71.9	72.4	73.8	74.1
CR/BP_After Aging	74.1	73.9	74.5	74.9	77.5	77.1

TABLE 7 Shore A hardness of the NR/BP composites and CR/BP composites at various basalt contents.

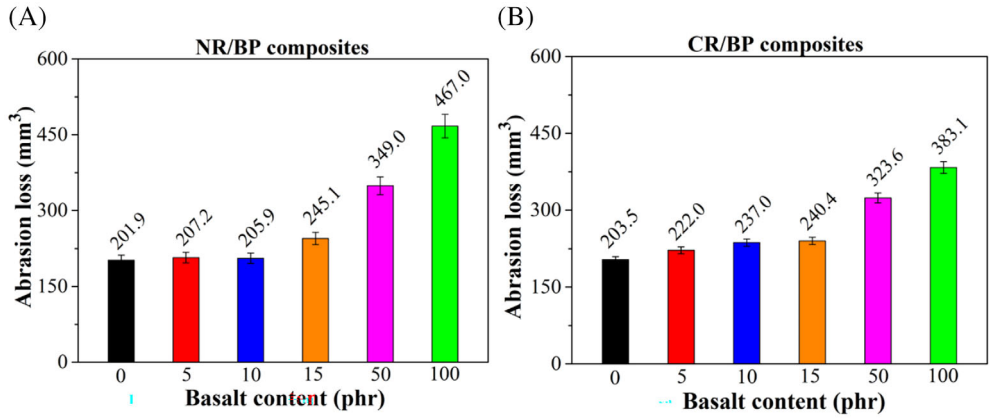

FIGURE 8 Abrasion loss at various basalt powder percentages of (A) NR/BP composites and (B) CR/BP composites.

a loading of 100 parts per hundred rubbers (phr), the hardness increases to 60.3. Similarly, the hardness of chloroprene rubber rises from 72 to 74.1 with the same basalt loading (Table 7). This increase in hardness can be attributed to the addition of more rigid basalt powder,[47] which affects the rubber's plasticity and elasticity, as illustrated in Figures 5 and 6. Although the NR composite experiences a modest hardness increase of about 9%, the CR composite shows a smaller rise of approximately 3% at the highest basalt loading. The hardness tends to decrease or remain relatively stable at loading levels from 5 to 15 phr, suggesting that basalt powder acts more as a filler than a reinforcement. After aging, the hardness of both NR/BP and CR/BP composites increases by 1%–11%. This finding aligns with research by Huang et al., which indicates that hydrothermal aging enhances crosslink density in rubber. This, in turn, leads to a more compact internal structure and improves the hardness of the samples.[48]

Figure 8 illustrates the comparative abrasion loss of NR/BP and CR/BP composites. Figure 8A presents the relationship between basalt content (phr) and the abrasion loss of NR/BP composites. As the basalt content increases, the hardness of the composites reinforced with 50 and 100 phr basalt powder also rises, as shown in Table 7. However, there is a significant decrease in abrasion resistance, indicated by an increase in abrasion loss. The abrasion loss for the composite with 0phr is 201.9 mm^3. This loss increases to 347 mm^3 at 50 phr and 467 mm^3 at 100 phr. Consequently, the abrasion loss of

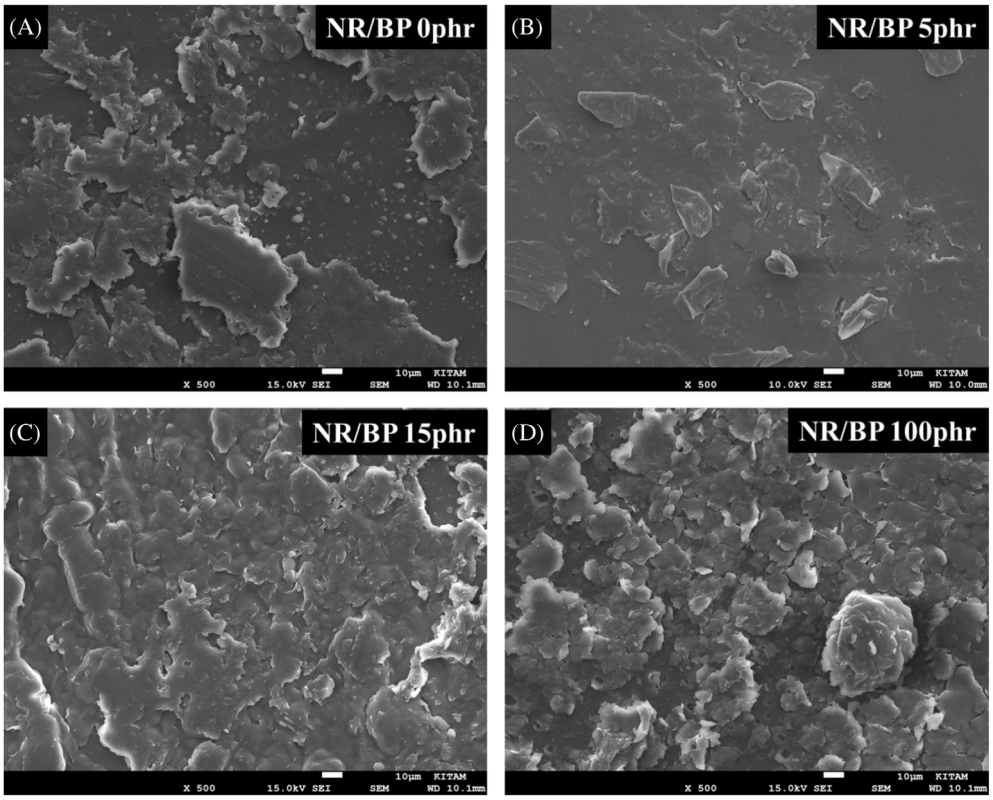

FIGURE 9 SEM images of natural rubber composites (A) NR/BP 0 phr, (B) NR/BP 5 phr, (C) NR/BP 15 phr, (D) NR/BP 100 phr.

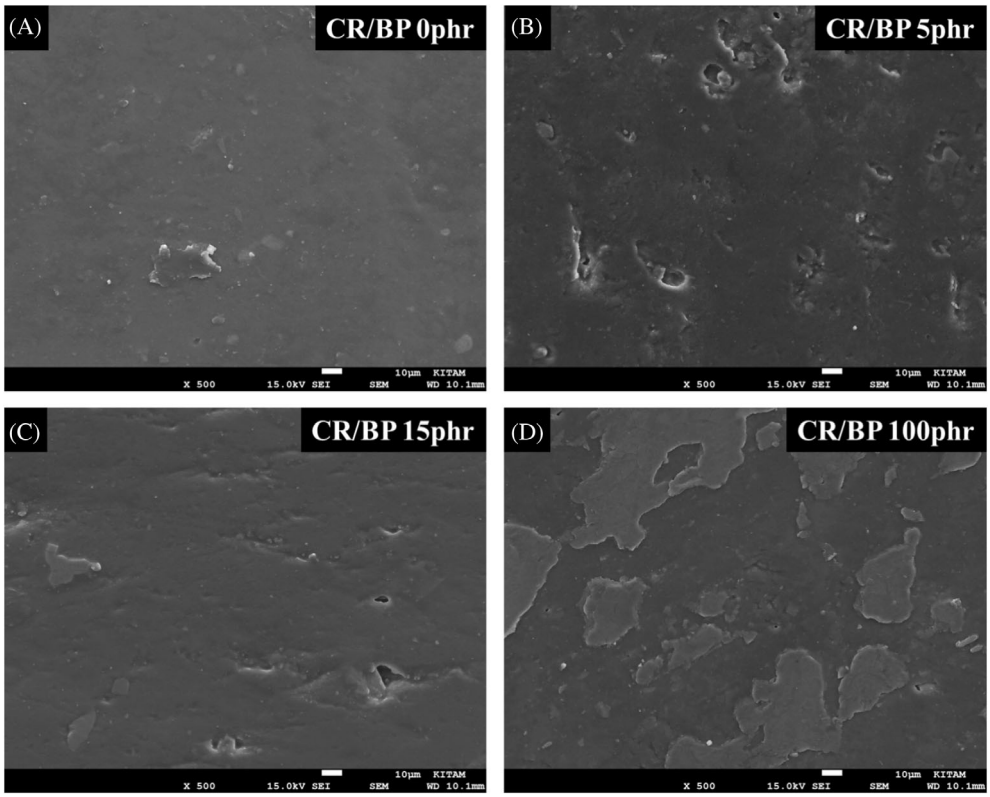

FIGURE 10 SEM images of polychloroprene rubber composites (A) CR/BP 0 phr, (B) CR/BP 5 phr, (c) CR/BP 15 phr, (D) CR/BP 100 phr.

NR/BP composites shows a 72% increase when reinforced with 50 phr of basalt content and a 130% increase when reinforced with 100 phr, compared to the pure NR matrix.

Furthermore, the abrasion loss of the CR matrix is precisely quantified to be 203.5 mm^3 (Figure 8B). When the basalt content is increased to 50 and 100 phr, the abrasion loss increases to 323.6 and

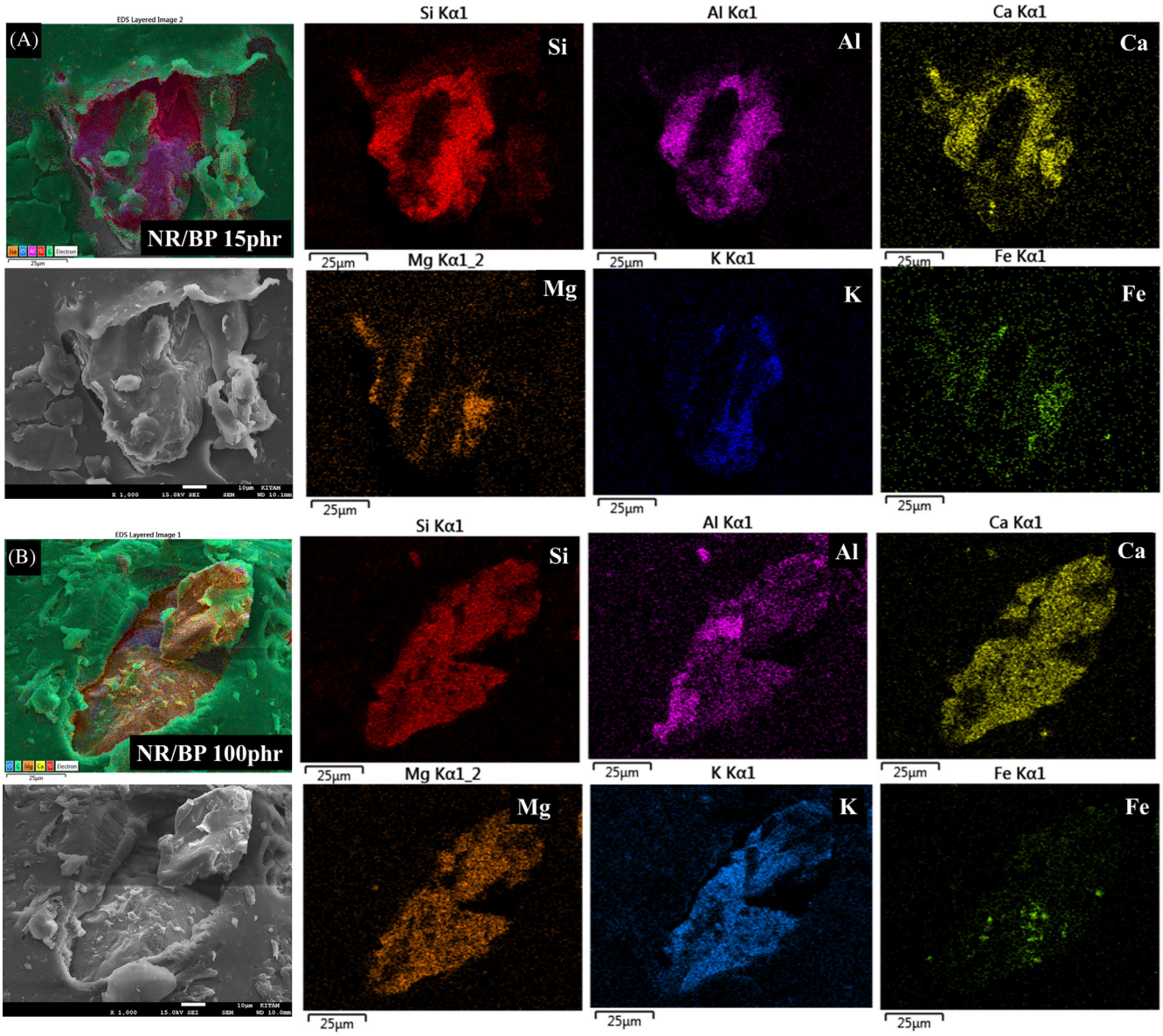

FIGURE 11 SEM–EDX photographs of NR composites (A) NR/BP 15 phr and (B) NR/BP 100 phr.

383.1 mm^3, respectively. Adding 50 and 100 phr basalt content to CR/BP composites increases abrasion loss by 59% and 88%, respectively, compared to the neat CR matrix. Including basalt powder increased abrasion loss, suggesting that adding basalt powder reduces the abrasion resistance of NR and CR composites. The higher abrasion ratio of the composites compared to pure NR and CR may be attributed to the inherent brittleness of basalt powders dispersed inside the rubber. Basalt powders possess a higher modulus and stiffness than natural and synthetic rubber, characterized by their toughness and ductility. The results indicate that basalt reinforcement has resulted in a more significant reduction in the abrasion loss of natural rubber compared to synthetic chloroprene rubber. This phenomenon can be attributed to the relatively weak interactions between the basalt reinforcements and the natural rubber matrix.

The inhomogeneous distribution of basalt becomes more pronounced at higher additive rates, forming agglomerations. Similar to its effect on mechanical properties, wear resistance is influenced by various factors, including the dimensions and configuration of the filler material, the quality of its dispersion, and the percentage of filler volume.[49,50] This study's findings suggest that the size, dispersion, and compatibility of basalt powder with the matrix have a more significant impact on wear properties than the hardness of the material.

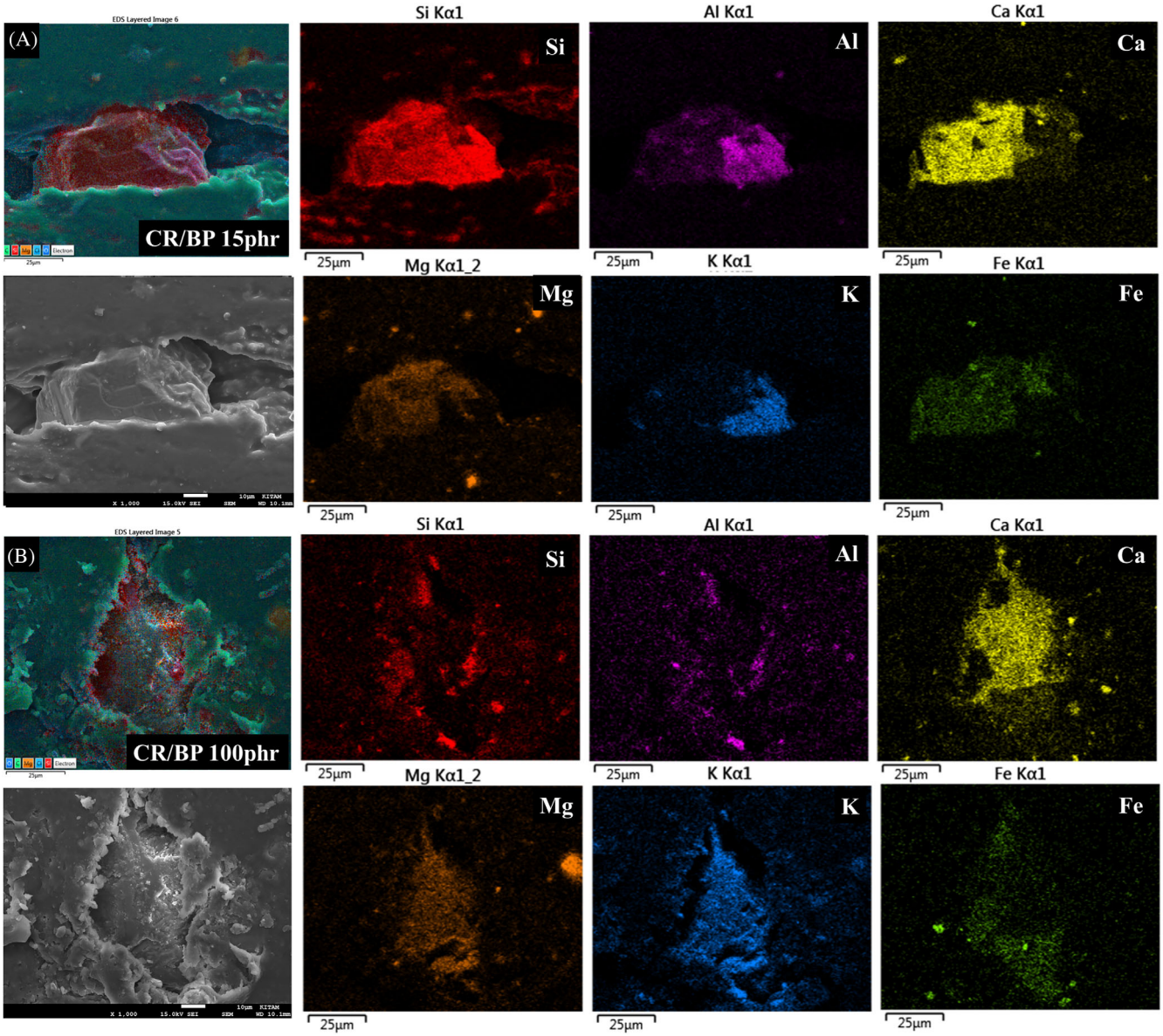

FIGURE 12 SEM–EDX photographs of CR composites (A) CR/BP 15 phr and (B) CR/BP 100 phr.

TABLE 8 Chemical compositions of the basalt.[18]

Composition	SiO_2	Al_2O_3	Fe_2O_3	CaO	MgO	TiO_2	Na_2O	Other
wt%	45–60	12–19	5–15	6–12	3–7	0, 9–2, 0	2, 5–6, 0	2, 0–3, 5

3.6 | Surface morphology of NR/BP and CR/BP composites

Figures 9 and 10 illustrate the surface morphology of NR/BP and CR/BP composites, respectively. The SEM images indicate that the surface of CR composites (Figure 10) is smoother than that of NR composites (Figure 9). This morphological difference depends on the amount of filler included in the composites.[51] The roughness of the cracked surfaces increases as the basalt powder loading rises from 5 to 100 phr. It is evident that a higher content of basalt powder negatively affects the dispersion of the filler. Figure 9D shows significant agglomeration when the loading reaches 100 phr. The SEM images demonstrate the matrix's filler distribution decreases as the basalt filler ratio increases. As mentioned earlier, the interactions between the filler and matrix weaken, leading to reduced values in tensile strength, Young's modulus, and abrasion resistance (Figures 5, 6, and 8).

Figures 11 and 12 illustrate the physical structure and distribution of chemical elements in basalt powder. Energy-dispersive X-ray spectroscopy was used to analyze the presence and dispersion of basalt powder on the fractured surfaces of the samples. The analysis software maps the elements detected in the SEM images. The EDX analysis confirms the incorporation of basalt powder in both the 15 and 100-phr reinforced natural rubber and chloroprene rubber composites, as verified by the mapped images.[52] While examining specific areas within the samples from which particles had been removed, the following elements were identified through EDX element mapping: Si^{+4}, Al^{+3}, Ca^{2+}, Mg^{2+}, K^{+}, and F^{+3}. As shown in Table 8, the chemical composition of basalt aligns with the elements identified in the EDX mapping. This confirms the presence of basalt in the structure of both NR and CR composites at varying contribution rates, further supported by the FTIR results (Figures 3 and 4).

4 | CONCLUSION

This study comprehensively analyzed the impact of basalt powder filler on the properties of natural rubber and polychloroprene rubber composites. The tensile strength was found to decrease with increasing basalt powder content both before and after aging; however, aged composites demonstrated higher tensile strength and Young's modulus due to increased crosslink density and the transformation of polysulfide bonds to disulfide bonds during aging. Additionally, the elongation at break values either decreased or remained constant with increasing basalt content, with aging having a limited impact, as the values were almost equal to or higher than the initial measurements. Furthermore, adding basalt increased the Shore A hardness of the NR/BP and CR/BP composites, which can be attributed to the tougher basalt reinforcements. Aging further increased the hardness values by 1%–11%, likely due to the elevated crosslink density. In conclusion, while basalt powder can effectively alter the mechanical properties of rubber composites, optimizing the filler content and fiber-matrix interface is crucial to balance enhanced properties with material integrity. Future research should focus on improving filler dispersion techniques and reinforcement-matrix adhesion through surface modifications of basalt reinforcements to mitigate the adverse effects observed at higher basalt loadings.

ACKNOWLEDGMENTS

This study was funded by the Scientific and Technological Research Council of Turkey (TUBITAK) Project Ref. No: 1139B412301068 Industry-Oriented Research Project Support Programme for Undergraduate Students (Project Ref. No: 1139B412301068). The authors would like to express their gratitude to the staff of the research and development department of Sampa Automotive Industry and Trade Inc. (Samsun, Türkiye) for their invaluable technical support.

DATA AVAILABILITY STATEMENT

The data that support the findings of this study are available from the corresponding author upon reasonable request.

ORCID

Volkan Eskizeybek https://orcid.org/0000-0002-5373-0379

Emine Feyza Sukur https://orcid.org/0000-0003-2644-880X

REFERENCES

1. Liu X, Shangguan W. Elastomeric components for noise and vibration isolation and control in the automotive industry. *Encycl Automot Eng*. 2014;1-17. doi:10.1002/9781118354179.auto160
2. Alarifi IM. A comprehensive review on advancements of elastomers for engineering applications. *Adv Ind Eng Polym Res*. 2023;6:451-464. doi:10.1016/j.aiepr.2023.05.001
3. Barrera C, Tardiff JL. Static and dynamic properties of eggshell filled natural rubber composites for potential application in automotive vibration isolation and damping. *J Clean Prod*. 2022;353:131656. doi:10.1016/j.jclepro.2022.131656
4. Parvathi K, Ramesan MT. Compliant materials based on nickel oxide/chlorinated natural rubber nanocomposites. *Polym Compos*. 2022;43:2628-2637. doi:10.1002/pc.26562
5. Sjöberg M, Kari L. Testing of nonlinear interaction effects of sinusoidal and noise excitation on rubber isolator stiffness. *Polym Test*. 2003;22:343-351. doi:10.1016/S0142-9418(02)00110-1
6. Chenal J, Gauthier C, Chazeau L, Guy L, Bomal Y. Parameters governing strain induced crystallization in filled natural rubber. *Polymer*. 2007;48:6893-6901. doi:10.1016/j.polymer.2007.09.023
7. Parvathi K, Al-Maghrabi MA, Subburaj M, T.Ramesan M. Natural rubber and copper alumina nanocomposite-based flexible elastomer-inorganic hybrid systems. *Polym Compos*. 2021;42:4586-4595. doi:10.1002/pc.26170
8. Parvathi K, Ramesan MT. Natural rubber composites filled with zinc ferrite nanoparticles: focus on structural, morphological, curing, thermal and mechanical properties. *Res Chem Intermed*. 2022;48:129-144. doi:10.1007/s11164-021-04586-5
9. Parvathi K, Verma M, Ramesan MT. Enhanced thermal, electrical and mechanical properties of nickel oxide reinforced chlorinated natural rubber/poly (indole) blend nanocomposites. *J Therm Anal Calorim*. 2023;148:10139-10149. doi:10.1007/s10973-023-12358-z
10. Burgaz E, Gencoglu O, Goksuzoglu M. Carbon black reinforced natural rubber/butadiene rubber and natural rubber/butadiene rubber/styrene-butadiene rubber composites: part I: rheological, mechanical and thermomechanical properties. *Res Eng Struct Mater*. 2019;5(3):233. doi:10.17515/resm2019.74ma1123
11. Barrera CS, Cornish K. Novel mineral and organic materials from agro-industrial residues as fillers for natural rubber. *J Polym Environ*. 2015;23:437-448. doi:10.1007/s10924-015-0737-4

12. Roy K, Debnath SC, Raengthon N, Potiyaraj P. Understanding the reinforcing efficiency of waste eggshell-derived nano calcium carbonate in natural rubber composites with maleated natural rubber as compatibilizer. *Polym Eng Sci*. 2019;59:1428-1436. doi:10.1002/pen.25127
13. Elfaleh I, Abbassi F, Habibi M, et al. A comprehensive review of natural fibers and their composites: an eco-friendly alternative to conventional materials. *Res Eng*. 2023;19:101271. doi:10.1016/j.rineng.2023.101271
14. Sunny T, Pickering K. An overview of alkali treatments of hemp fibres and their effects on the performance of polymer matrix composites. *Alkal Chem Appl*. 2021;3. doi:10.5772/intechopen.100321
15. Ulus H, Kaybal HB, Eskizeybek V, Avcı A. Enhanced salty water durability of halloysite nanotube reinforced epoxy/basalt fiber hybrid composites. *Fibers Polym*. 2019;20:2184-2199. doi:10.1007/s12221-019-9316-y
16. Sukur EF, Onal G. Graphene nanoplatelet modified basalt/epoxy multi-scale composites with improved tribological performance. *Wear*. 2020;460–461:203481. doi:10.1016/j.wear.2020.203481
17. Ulus H, Kaybal HB, Eskizeybek V, Avcı A. Halloysite nanotube reinforcement endows ameliorated fracture resistance of seawater aged basalt/epoxy composites. *J Compos Mater*. 2020;54:2761-2779. doi:10.1177/0021998320902821
18. Sukur EF, Onal G. Long-term salt-water durability of GNPs reinforced basalt-epoxy multiscale composites for marine applications. *Tribol Int*. 2021;158:106910. doi:10.1016/j.triboint.2021.106910
19. Ma H, Wang B, Gao W, Liu D, Sun Y, Liu Z. Optimal scheduling of a regional integrated energy system with energy storage systems for service regulation. *Energies*. 2018;11:195. doi:10.3390/en11010195
20. Zhu D, Wang C, Han D. Investigating the effect of different amounts of basalt fiber (BF) during the mixing process on metal friction and wear. *Polym Test*. 2022;115:107750. doi:10.1016/j.polymertesting.2022.107750
21. Wu W, Zuo H. Silicone rubber composites modified by chopped basalt fibers treated with coupling agent. *SILICON*. 2018;10:2555-2559. doi:10.1007/s12633-018-9790-7
22. Wu WL, Feng HH. Study on short basalt fiber reinforced fluorine rubber composites. *Adv Mater Res*. 2014;1052:258-261. doi:10.4028/www.scientific.net/AMR.1052.258
23. Li Z, Wan J, Li Y, Li Y, Zhao F, Zhao S. Effects of coupling agents on the properties of an NR/SBR matrix and its adhesion to continuous basalt fiber cords. *J Appl Polym Sci*. 2019;136:47098. doi:10.1002/app.47098
24. Rybiński P, Syrek B, Żukowski W, et al. Impact of basalt filler on thermal and mechanical properties, as well as fire hazard, of silicone rubber composites, including ceramizable composites. *Materials*. 2019;12:2432. doi:10.3390/ma12152432
25. Rybiński P, Syrek B, Marzec A, et al. Effects of basalt and carbon fillers on fire hazard, thermal, and mechanical properties of EPDM rubber composites. *Materials*. 2021;14:5245. doi:10.3390/ma14185245
26. Kuru G, Goksuzoglu M, Ak EC, Arabacı TN. The effect of acetylene black amount, operating pressure and temperature of capillary rheometer on thermal conductivity in natural rubber. *Plast Rubber Compos*. 2023;52:276-291. doi:10.1080/14658011.2023.2197679
27. Kuru G, Goksuzoglu M. Investigating pyrolytic carbon black in natural rubber compounds: rheological, mechanical and dynamic effects. *J Rubber Res*. 2024. doi:10.1007/s42464-024-00292-0
28. Surya I, Sukeksi L, Hayeemasae N. Studies on cure index, swelling behaviour, tensile and thermooxidative properties of natural rubber compounds in the presence of alkanolamide. *IOP Conf Ser Mater Sci Eng*. 2018;309:012060. doi:10.1088/1757-899X/309/1/012060
29. Nabil H, Ismail H, Azura AR. Compounding, mechanical and morphological properties of carbon-black-filled natural rubber/recycled ethylene-propylene-diene-monomer (NR/R-EPDM) blends. *Polym Test*. 2013;32:385-393. doi:10.1016/j.polymertesting.2012.11.003
30. Martínez JD, Cardona-Uribe N, Murillo R, García T, López JM. Carbon black recovery from waste tire pyrolysis by demineralization: production and application in rubber compounding. *Waste Manag*. 2019;85:574-584. doi:10.1016/j.wasman.2019.01.016
31. Urrego-Yepes W, Cardona-Uribe N, Vargas-Isaza CA, Martínez JD. Incorporating the recovered carbon black produced in an industrial-scale waste tire pyrolysis plant into a natural rubber formulation. *J Environ Manag*. 2021;287:112292. doi:10.1016/j.jenvman.2021.112292
32. Du A, Wu M, Su C, Chen H. The characterization of pyrolytic carbon black prepared from used tires and its application in styrene–butadiene rubber (SBR). *J Macromol Sci Part B*. 2008;47:268-275. doi:10.1080/00222340701748768
33. Li Z, Li Y, Cheng J, Lu X, Yang Y. Effects of fibre content and orientation on wear properties of basalt fibre/acrylonitrile–butadiene rubber composites. *Iran Polym J*. 2020;29:361-367. doi:10.1007/s13726-020-00802-y
34. Intapun J, Rungruang T, Suchat S, Cherdchim B, Hiziroglu S. The characteristics of natural rubber composites with klason lignin as a green reinforcing filler: thermal stability, mechanical and dynamical properties. *Polymers*. 2021;13:1109. doi:10.3390/polym13071109
35. Ambilkar SC, Dhakar GL, Kapgate B, et al. Enhancing the material performance of chloroprene rubber (CR) by strategic incorporation of zirconia. *Mater Adv*. 2022;3:2434-2446. doi:10.1039/D1MA00793A
36. Košíková B, Gregorová A, Osvald A, Krajčovičová J. Role of lignin filler in stabilization of natural rubber–based composites. *J Appl Polym Sci*. 2007;103:1226-1231. doi:10.1002/app.24530
37. Nazir MT, Phung BT, Yeoh GH, et al. Enhanced dielectric and thermal performance by fabricating coalesced network of alumina trihydrate/boron nitride in silicone rubber for electrical insulation. *Bull Mater Sci*. 2020;43:220. doi:10.1007/s12034-020-02201-8
38. Kurbonov A, Sattorov L, Kamolov B, Rakhimov O. Chemical and mineralogical studies of basalt "Aydarkul". *BIO Web Conf*. 2023;71:2040. doi:10.1051/bioconf/20237102040
39. Ginting EM, Bukit N, Motlan, Saragih MT, Frida E, Bukit BF. Analysis of natural rubber compounds with filler of oil palm empty bunches powder and carbon black. *J Phys Conf Ser*. 2020;1428:012024. doi:10.1088/1742-6596/1428/1/012024
40. Rahmah M, Ahmad Khusyairi AR, Nur Khairunnisya H, Siti Nurbalqis M. Oven ageing versus UV ageing properties of natural rubber cup lump/EPDM rubber blend with mangosteen

powder (MPP) as natural antioxidant. *IOP Conf Ser Mater Sci Eng*. 2019;548:012014. doi:10.1088/1757-899X/548/1/012014
41. Prasath KA, Arumugaprabu V, Amuthakkannan P, Manikandan V, Deepak Joel Johnson R. Low velocity impact, compression after impact and morphological studies on flax fiber reinforced with basalt powder filled composites. *Mater Res Express*. 2020;7:015317. doi:10.1088/2053-1591/ab611e
42. Rolere S, Liengprayoon S, Vaysse L, Sainte-Beuve J, Bonfils F. Investigating natural rubber composition with Fourier transform infrared (FT-IR) spectroscopy: a rapid and non-destructive method to determine both protein and lipid contents simultaneously. *Polym Test*. 2015;43:83-93. doi:10.1016/j.polymertesting.2015.02.011
43. Wu W, Yu B. The mechanical and thermal properties of KH590-basalt fibre-reinforced silicone rubber/fluorine rubber composites. *J Rubber Res*. 2020;23:163-171. doi:10.1007/s42464-020-00046-8
44. Kun L, Xin LH, Bei LB, Nan LY. Mechanical performance and carbonation resistance of basalt fiber—polypropylene fiber rubber concrete. *Front Mater*. 2023;10:10. doi:10.3389/fmats.2023.1229629
45. Kong Y, Chen X, Li Z, Li G, Huang Y. Evolution of crosslinking structure in vulcanized natural rubber during thermal aging in the presence of a constant compressive stress. *Polym Degrad Stab*. 2023;217:110513. doi:10.1016/j.polymdegradstab.2023.110513
46. Longkaew K, Gibaud A, Tessanan W, Daniel P, Phinyocheep P. Spherical $CaCO_3$: synthesis, characterization, surface modification and efficacy as a reinforcing filler in natural rubber composites. *Polymers*. 2023;15(21):4287. doi:10.3390/polym15214287
47. Mente P, Tshwafo M. Natural rubber and reclaimed rubber composites–a systematic review. *Pol Sci*. 2016;2:2. doi:10.4172/2471-9935.100015
48. Huang G, Chen Z, Wu J, et al. Effect of hydrothermal aging on the tribological performance of nitrile butadiene rubber seals. *Polymers*. 2024;16(1):81. doi:10.3390/polym16010081
49. Pal K, Pal SK, Das CK, Kim JK. Effect of fillers on morphological and wear characteristics of NR/HSR blends with E-glass fiber. *Mater Des*. 2012;35:863-872. doi:10.1016/j.matdes.2011.07.074
50. Damircheli M, MajidiRad A. The influence of the dispersion method on the morphological, curing, and mechanical properties of NR/SBR reinforced with nano-calcium carbonate. *Polymers*. 2023;15(13):2963. doi:10.3390/polym15132963
51. Shaniba V, Sreejith MP, Aparna KB, Jinitha TV, Purushothaman E. Mechanical and thermal behavior of styrene butadiene rubber composites reinforced with silane-treated peanut shell powder. *Polym Bull*. 2017;74:3977-3994. doi:10.1007/s00289-017-1931-4
52. Anand A, Nussana L, Sham Aan MP, Ekwipoo K, Sangashetty SG, Jobish J. Synthesis and characterization of ZnO nanoparticles and their natural rubber composites. *J Macromol Sci Part B*. 2020;59:697-712. doi:10.1080/00222348.2020.1798097

SUPPORTING INFORMATION

Additional supporting information can be found online in the Supporting Information section at the end of this article.

How to cite this article: Yildiz E, Degirmenci T, Esen M, et al. Impact of basalt powder on the rheological, thermal, mechanical, and tribological properties of natural and polychloroprene rubber composites: A study on aging and filler interaction. *Polym Compos*. 2025;1-18. doi:10.1002/pc.29706